Journal of Non-Crystalline Solids: X 1 (2019) 100012

Contents lists available at ScienceDirect

Journal of Non-Crystalline Solids: X

journal homepage: www.journals.elsevier.com/journal-of-non-crystalline-solids-x

Pentacoordinated silicon in ambient pressure potassium and lithium silicate glasses: Temperature and compositional effects and analogies to alkali borate and germanate systems

Jonathan F. Stebbins*

Department of Geological Sciences, Stanford University, Stanford, CA, USA

ARTICLE INFO

Keywords:
Nuclear magnetic resonance
NMR
Five coordinated silicon
Fictive temperature
Alkali borate glass
Alkali germanate glass

ABSTRACT

Pentacoordinated silicon (SiO_5) has long been considered as a possible reactive intermediate in bond-swapping reactions in even ambient pressure viscous flow, diffusion, nucleation and crystallization. In this paper, new results are presented for potassium silicate glasses and for two lithium silicates. In the former, SiO_5 is readily detectable by ^{29}Si MAS NMR on ^{29}Si-enriched glasses at concentrations as low as about 0.02 mol%; in the latter this species is below detection limits. SiO_5 concentrations are higher at higher fictive temperatures, and first increase, then decrease, as K_2O is added to SiO_2. This pattern in compositional variation resembles those long-known in alkali borate and germanates, although high coordinate species (BO_4 and GeO_5/GeO_6) are orders of magnitude more abundant than in ambient pressure silicates. A simple thermodynamic model, considering only the non-ideal mixing of bridging and non-bridging oxygens, at least qualitatively predicts the shape of the compositional variation of SiO_5 in the potassium silicates, and is sensible with respect to known tendencies for clustering and unmixing; such a model also predicts curves of network cation coordination vs. compositon that resemble those known for borates and germanates, suggesting an underlying similarity in the energetics of mixing of anionic species.

1. Introduction

Tetrahedrally coordinated silicon (SiO_4) is the archetypical former of network structures in silicate crystals and glasses. With the exceptions of one known calcium silicate hydrate (thaumasite) and crystalline and glassy phosphosilicates [1–6], all or nearly all silicon in ambient pressure silicates is in SiO_4 groups. Higher coordinated silicon species (penta- and hexacoordinated silicon, SiO_5 and SiO_6 in the context of oxides) are usually considered to be structurally significant only in high pressure silicates, and indeed the latter species is probably the most important form of Si in the deep Earth, in the perovskite-structured (Mg,Fe)SiO_3 phase (bridgmanite) that makes up most of the planet's lower mantle.

SiO_5 groups were first discovered in high pressure alkali silicate glasses by ^{29}Si NMR almost 30 years ago, reaching concentrations of up to about 4 to 8 M % in $Na_2Si_4O_9$ and $K_2Si_4O_9$ glasses quenched from melts at 6 to 12 GPa (60 to 120 kbar), decompressed, and studied under ambient conditions [7–9]. Very low concentrations of this species (ca. 0.1%) were then detected by the same methods in several 1 bar glasses of these compositions [10,11]. Cooling rate experiments demonstrated its increasing abundance at higher fictive temperature (T_f). A few more recent studies of high pressure glasses have confirmed and extended these results [12–15], but the expense of the isotopically enriched ^{29}Si that has generally been required has limited the exploration of compositional effects on Si coordination, potentially one of the most fundamental aspects of the network structure of silicate glasses.

We have recently begun a program to improve and expand these results, with an initial study that showed that SiO_5 and SiO_6 concentrations in high pressure $K_2Si_4O_9$ glasses may be considerably higher than previously thought, due to transient pressure drop effects on quench from super-liquidus temperatures in solid-media high pressure apparatuses [16,17]. That new study also confirmed the fictive temperature effect on SiO_5 content at 1 bar pressure in this one composition. The obtainable signal-to-noise ratios for small samples have improved considerably since early work, with faster spinning MAS NMR probes and higher external magnetic fields, making systematic explorations of this species considerably more feasible. This is true even for the low concentrations of SiO_5 in 1 bar glasses, in which complications of high pressure experiments such as pressure control, uncertain thermal history, and, potentially, structural changes during

* Corresponding author.
E-mail address: stebbins@stanford.edu.

https://doi.org/10.1016/j.nocx.2019.100012
Received 20 November 2018; Received in revised form 17 January 2019; Accepted 18 January 2019
Available online 19 February 2019

Table 1
Concentrations of SiO_5 groups in alkali silicate glasses (molar % of total Si) and apparent enthalpies for reaction (1). Experimental uncertainties in SiO_5 contents are about 10 to 20% relative.

Mole % M_2O	Fast quench SiO_5	Fast quench, est. T_f, K	Slow cooled SiO_5	Slow cooled, est. T_f, K	ΔH_{app} kJ/mol[b]	ΔH_{app} kJ/mol non-ideal model[c]
5% K_2O	0.23	1125	0.10[a]	909	–	13
10% K_2O	0.35	989	0.20	813	22	19
15% K_2O	0.26	959	0.11	793	33	25
20% K_2O	0.10	930	0.05	773	26	30
25% K_2O	0.03	923	–	–	–	36
20% Li_2O	n.d.[d] (< 0.04%)					
33% Li_2O	n.d. (< 0.02%)					

[a] Slow-cooled 5% K_2O sample contained about 20–30% crystalline silica, pushing glass composition to about 6 to 7% K_2O. ΔH_{app} is not given here because of this additional uncertainty in effects on thermal history.
[b] Calculated from experimental data for fast quench and slow cooled glasses.
[c] Effects of composition on ΔH_{app} as calculated from non-ideal solution model for NBO activities, with interaction parameter W = 60 kJ/mol, and starting value for ΔH_{app} fixed at 30 kJ/mol for 20% K_2O. See text in Section 4.1.
[d] "n.d." indicates not detected in NMR spectra.

decompression, can be eliminated. Here are presented the results of the first extensive study of silica content on silicon coordination in any simple silicate binary.

Such a low-abundance silicate species in ambient pressure glasses may appear to be a curiosity or a minor correction to standard structural models. However, SiO_5 groups, since early work on molecular dynamics simulations of silicate melt dynamics [18,19], have been implicated in mechanisms not only by which structure changes with pressure, but in how the breaking and re-forming of strong network bonds (bond swapping) takes place as quantified by in-situ high temperature NMR [20,21]. The latter process is thought to be important for network cation (and anion) diffusion and viscous flow in at least high-silica liquids [22–25], and has been the subject of numerous recent theoretical studies [26–33]. Here, as well as in some models of silicate dynamics in other contexts including aqueous dissolution and crystallization [34–37], low concentrations of over-coordinated Si may serve as "transition complexes" that are critical to kinetics.

A second type of motivation to improving the scope of data on SiO_5 groups in silicate glasses concerns apparently fundamental differences in the interactions of composition, structure and properties in the three classical oxide glass forming systems: silicates, borates, and germanates. These are all best known through effects of addition of alkali oxides (M_2O) to the pure oxides SiO_2, B_2O_3, and GeO_2, as these systems have the widest range of glass forming compositions for which liquid-liquid phase separation (at low M_2O) and crystallization (at high M_2O) can be avoided. In low-pressure silicates, the predominant silicon coordination is largely unaffected by addition of alkali oxides, and properties of both glasses and liquids, such as density (or molar volume), refractive index, and glass transition temperature vary either linearly with composition or at least monotonically as bridging oxygens are converted to non-bridging oxygens, often allowing simple parameterization [38]. In marked contrast, variations in properties with composition in the alkali borate and alkali germanate binary systems are often non-linear and even non-monotonic, e.g. molar volumes in both glasses and liquids [39] and observations that T_g may increase to a maximum then decrease with further addition of M_2O [40–42]. A number of structural explanations of such "anomalous" behaviors have been proposed and extensively studied by spectroscopy, X-ray and neutron scattering, but most involve the initial conversion of the network cation groups (BO_3 or GeO_4) to higher coordination (BO_4 or GeO_5/GeO_6) with M_2O addition, with little or no formation of NBO. Effects on properties are thus drastically different than in silicate systems. After reaching maxima, boron and germanium cation coordinations then are converted back to the lower coordination state at higher M_2O concentrations. In silicates at high pressure when SiO_5 (and SiO_6) groups become stable enough to have concentrations similar to those of SiO_4, such complex behavior might be expected, but few or no data are available on either structure or properties of binary composition liquids under such conditions. Ambient pressure compositional effects on SiO_5 contents may thus provide some clues to high pressure property behavior by analogy to borates and germanates [9,42]. Intriguingly, the results and their analysis in simple thermodynamic terms as presented here for potassium silicates also suggest that this system may yield new insights into the underpinnings of cation coordination changes that are known so much more completely in the borates and germanates.

2. Experimental methods

2.1. Glass synthesis

As described in our recent paper on high pressure $K_2Si_4O_9$ glasses [17], glasses studied here were made from either 99% or ca. 60% ^{29}Si enriched silica and high purity anhydrous K_2CO_3 or Li_2CO_3, melted in batches of 100 to 700 mg in a Pt/Au crucible after an initial decarbonation step at ca. 700 °C. Melting was typically done for 1 h at 50 to 100 °C above liquidus temperatures. Given the small sample sizes necessitated by the expense of the isotopically enriched starting material, several compositions were made by adding either $^{29}SiO_2$ or alkali to a previous sample. Trace element dopants, added to speed spin-lattice relaxation, varied somewhat. The 20% K_2O glass, and compositions derived from it (15% and 25% K_2O) contained about 0.2 wt% Gd_2O_3 in order to match the samples of an early study [9], as well as traces of transition metal contaminants in the silica [43]. The 5% K_2O glass, the subsequent 10% K_2O sample, and the Li silicates were doped with 0.1 to 0.2 wt% CoO. Compositions (Table 1) are nominal, but controls on weight loss during melting indicate that these are accurate to within 1 or 2% absolute.

All samples were initial rapidly quenched from above the liquidus by dipping the crucible base into water, forming a layer of glass typically < 1 mm thick at a rate estimated to be roughly 500 to 1000 K/s (fast quenched or "FQ" designation). Portions of glasses with 10, 15 and 20% K_2O were then reheated to about 25 to 50 °C above their reported glass transition temperatures for about 30 min, then cooled slowly at 10 or 15 K/h to well below T_g (slowly cooled or "SC" designation), also as described recently for the 20% composition, or $K_2Si_4O_9$. For the latter, the "SC" glass was then remelted and fast quenched again to demonstrate reversibility of fictive temperature effects [17]. In contrast, a portion of the FQ 5% K_2O glass was re-heated to about 100 °C above its T_g and then slow cooled, resulting in the formation of about 20–30% of a crystalline silica phase (probably tridymite) that was readily

detectable by NMR. None of the other samples showed any signs of crystallization: all were optically clear and bubble-free and showed no narrow crystal-like peaks in NMR spectra. Only the 20% Li_2O glass ($Li_2Si_4O_9$) showed any sign of liquid-liquid-phase separation, manifested as pronounced differential spin-lattice relaxation between SiO_4 species (see below), as expected from previous work on this composition [44]. Annealing/slow cooling experiments were not done on the 25% K_2O glass or the Li silicates, because initial NMR spectra showed either very low (25% K_2O) or undetectable (Li silicates) SiO_5 concentrations (see below).

2.2. NMR spectroscopy

^{29}Si NMR spectra were collected with a Varian Inova spectrometer at a field of 14.1 T and a frequency of 119.14 MHz, using a Varian/Chemagnetics T3 magic angle spinning probe with 3.2 mm zirconia rotors, typical spinning rates of 20 kHz, and sample weights of about 30 to 35 mg. One-pulse acquisition was used, with RF tip angles of about 30° (1 μs pulses). Frequencies are referenced to tetramethyl silane (TMS). Spectra were collected with pulse delays ranging from 0.1 to 3600 s as part of an ongoing, in-depth study of line shapes and relaxation. Gaussian apodization (smoothing of the time-domain signal) was limited to values that did not noticeably broaden spectra. In general, data shown here were chosen to optimize signal-to-noise ratios (1500 to 6000:1) needed to accurately measure tiny concentrations of SiO_5 groups, typically with a 4 s delay and relaxation to about 65% of fully relaxed intensity. Spectra shown typically sum data from 10,000 to 40,000 acquisitions, requiring about 12 to 44 h to collect. SiO_5 results are given as molar percentages of total silica, and are derived as previously described by direct integration of the spectra with a linear baseline interpolation for simplicity of data analysis [17]. These data are, within uncertainties, independent of the pulse delay used, for spectra in which signal-to-noise is high enough for accurate detection of such low concentrations.

3. Results and discussion

3.1. NMR spectra: SiO_4 regions

^{29}Si MAS NMR spectra for the glasses, showing the regions for the predominant SiO_4 species, are shown in Figs. 1 and 2. Lineshapes and positions are similar to those reported in a number of previous studies [45–48], but with signal-to-noise ratios greatly improved by the isotopic enrichment. In this composition range, the potassium silicate glasses all show two partially resolved peaks due to Q^3 and Q^4 sites: SiO_4 groups with 3 or with 4 bridging oxygens, centered at about −95 to −98 ppm and −105 to −110 ppm respectively. As expected from previous studies, the lithium silicate spectra also contain a lower Q^2 shoulder centered at about −80 ppm (Fig. 2). Q^3 and Q^4 peaks move systematically to slightly lower frequencies (more negative chemical shifts) with decreasing alkali oxide content, also as previously reported [46–48]. The size of the Q^4 peak relative to that of the Q^3 peak increases as expected with higher silica contents. However, in detail, we note that as in other recent studies, simple fitting with two Gaussian components does not give results fully consistent with composition in this range, requiring area-constrained fitting [48], the addition of a third peak to represent distinct Q^4 environments [47], or the possibility of asymmetric, non-Gaussian lineshapes.

In general, for silicate glasses doped with paramagnetic impurities to enhance relaxation and obtainable signal-to-noise ratios, lineshapes (and thus derived SiO_4 speciation) have been found to be independent of pulse delay, i.e. that all components relax at the same rate. In contrast, glasses with phase separation, even at the sub-optical scale, show markedly slower relaxation of Q^4 species, as these are concentrated in the high-silica phases that exclude most dopant cations (e.g. transition metals and rare earths) [44,49]. The result is that the Q^4 peak is

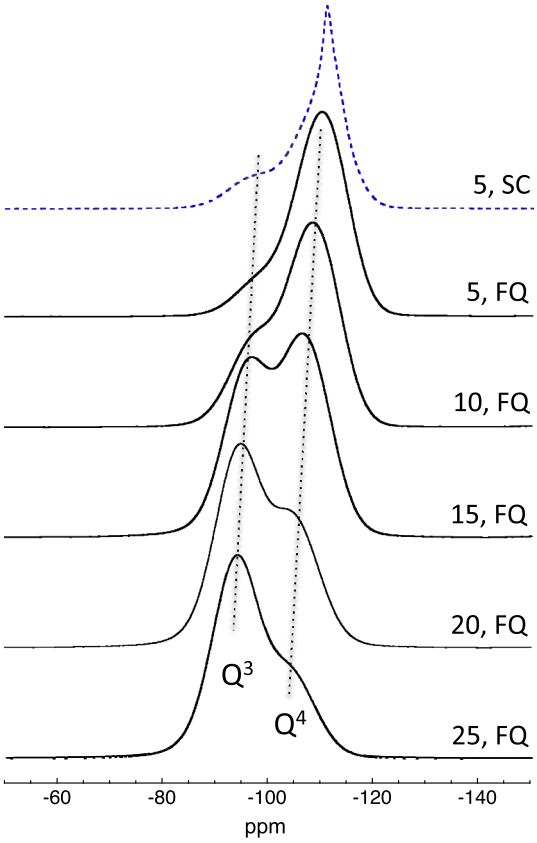

Fig. 1. ^{29}Si MAS NMR spectra for ^{29}Si-enriched K_2O-SiO_2 glasses, showing SiO_4 regions, with mole % K_2O as labeled. "FQ" designates "fast quenched"; "SC" designates "slowly cooled". All data shown were collected with a 4 s pulse delay. Uppermost spectrum (dashed curve) shows data for the slowly cooled 5% K_2O glass, which formed a minor amount of a crystalline silica phase during cooling from ca. 100 °C above T_g (see text).

underrepresented in spectra collected with pulse delays short enough to partially saturate the magnetization. This distinction is illustrated here (Fig. 2) by selected spectra for 20% Li_2O glass, with pronounced differential relaxation, contrasting with data for 33% Li_2O glass with no detectable change in lineshape with pulse delay. The former composition lies within the spinodal, which is well above the glass transition and thus leads to phase separation regardless of quench rate; the latter lies outside of the solvus. The very high signal-to-noise ratios obtainable here also suggest a slight differential relaxation for most of the K-silicate glasses, which are not known to phase separate, as the solvus in this binary apparently is below T_g for all compositions [50,51]. This finding suggests some heterogeneity in the distribution of paramagnetic dopant ions, even in single-phase glasses. Detailed analysis of MAS and static (non-spinning) lineshapes, as well as spin-lattice relaxation curves, will be presented in a future contribution.

For all glasses except the 5% K-silicate, annealing and slow cooling of the original fast-quenched samples had only very subtle effects on the SiO_4 lineshapes, typically with a slight narrowing of component peaks and a slight (< 0.5 ppm) shift down in frequency (Fig. 2a). These effects were completely reversible when tested in the 20% K_2O composition. Changes in Q species abundance with temperature and with fictive temperature, known to occur in lower silica compositions [52,53], are small enough to be negligible in the composition range explored here: e.g. the 20% K_2O glass probably contains only a few % Q^2 groups at most. Effects on SiO_5 concentrations of thermal history are, in contrast, large and significant (see below). For the 5% K_2O glass, which was heated much farther above T_g than for the other compositions for the slow cooling (SC) experiment, partial crystallization occurred to form a

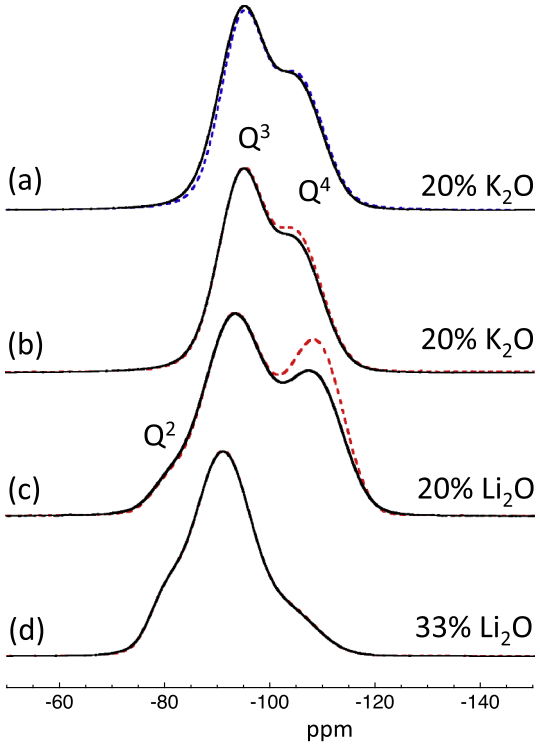

Fig. 2. ^{29}Si MAS NMR spectra for ^{29}Si-enriched K_2O-SiO_2 and Li_2O-SiO_2 glasses, showing SiO_4 regions, as labeled. For all, solid lines show data for fast-quenched glasses with pulse delays of 4 s. In (a), data for the slowly-cooled (SC) glass is shown with the superimposed dashed curve (blue). In (b), (c), and (d), data for fast-quenched glasses with pulse delays of 300, 300, and 60 s respectively are shown in superimposed (red) dashed curves, illustrating the presence of obvious differential relaxation between the Q^3 and Q^4 peaks (c) or its complete absence (d). For (b), (c), and (d), spectra are normalized to the same height for the Q^3 peak. The longer-delay spectra are fully or nearly-fully relaxed, the shorter-delay spectra are 66, 24, and 48% relaxed respectively. (For interpretation of the references to colour in this figure legend, the reader is referred to the web version of this article.)

narrower Q^4 component in the spectrum, centered at about −111 ppm (Fig. 1, top). This phase is probably a polymorph of tridymite, which because of its structural complexity has multiple, partially overlapping ^{29}Si NMR peaks and thus can give relatively broad overall lineshapes [54,55]. From the estimated content of this phase (20–30% of the observed ^{29}Si signal with a pulse delay of 1 h), the glass composition after this slow cooling experiment was probably enhanced somewhat in K_2O, to about 6 to 7%.

3.2. NMR spectra: SiO_5 regions

In Fig. 3, spectra are plotted with vertical scales enlarged by about 40 times over those shown in Figs. 1 and 2. As first discovered in early studies of the $K_2Si_4O_9$ composition (20% K_2O) [7,9,10] and recently re-confirmed [17], the very high signal-to-noise ratios obtainable with isotopically enriched ^{29}Si enable low concentrations of SiO_5 groups to be detected as peaks near to −150 ppm. Measured SiO_5 concentrations (Table 1) are highest in the 10% K_2O glass, and decrease at both lower and higher K_2O contents. The SiO_5 peak shifts slightly and progressively down in frequency (2 to 3 ppm more negative chemical shift) from the 25% to the 5% K_2O glass, possibly because of a shift in the number of bridging vs. non-bridging oxygen neighbors. The latter is suggested by the partial resolution of what may be two SiO_5 peaks in a 3 GPa pressure glass containing in total 2.4% of the species [17]. No signals for SiO_6 groups at ca. –200 ppm were detected in any of these samples, with a detection limit in most cases of about 0.02%. This species is well-

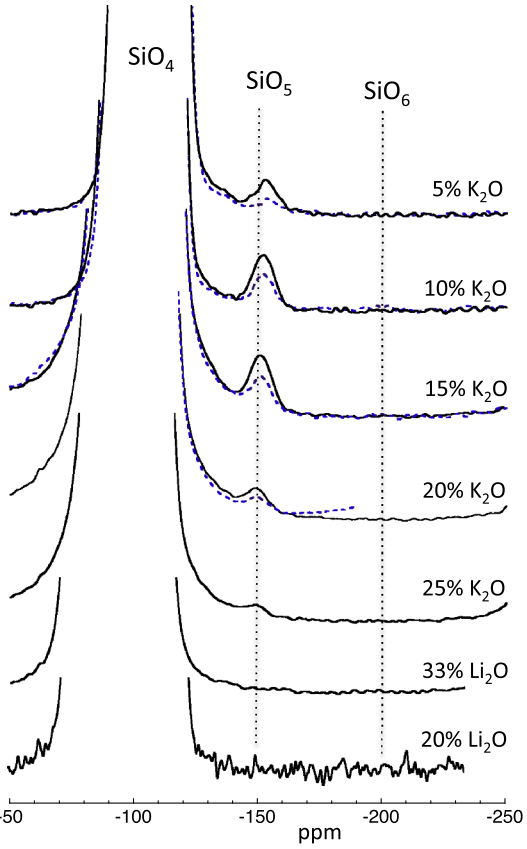

Fig. 3. ^{29}Si MAS NMR spectra for ^{29}Si-enriched K_2O-SiO_2 and Li_2O-SiO_2 glasses, showing SiO_4, SiO_5, and SiO_6 regions, as labeled. Vertical scales are expanded by about 40 times those in Figs. 1 and 2. The SiO_5 peak location is marked with a vertical line to illustrate small changes with composition. The SiO_6 peak location is based on data for high pressure glasses: this species is not detectable in these ambient-pressure glasses. Solid curves show data for fast-quenched glasses with pulse delays of 4 s (except 60 s for 20% Li_2O); dashed (blue) spectra show results for slowly-cooled glasses. The baseline of the latter spectrum for 20% K_2O curves upward at its low-frequency end because data were collected with a sample spinning rate of 14 instead of 20 kHz, giving a spinning sideband (not shown for clarity) at ca. –200 ppm [17]. (For interpretation of the references to colour in this figure legend, the reader is referred to the web version of this article.)

known from glasses formed at pressure of 1.5 GPa and above [7,17] as well as ambient-pressure phosphate-rich silicate glasses [2–5].

For the 5, 10, 15, and 20% K_2O glasses, for which portions of the original fast-quenched samples were annealed and cooled slowly through T_g, the SiO_5 peak is markedly reduced, as seen in early work [10,11] and as recently re-confirmed for the 20% composition [17]. The SiO_5 content (0.03%) for the FQ 25% K_2O glass was just above the detection limit, while those for the Li-silicates were below detection. The relatively slow spin-lattice relaxation of the phase-separated 20% Li_2O glass resulted in considerably lower practically obtainable signal-to-noise ratios and a higher SiO_5 detection limit of about 0.04%.

3.3. Observed compositional variation in SiO_5 concentration, formation mechanism, and correction for temperature effects

For both fast quenched and slowly-cooled K-silicate samples, measured SiO_5 contents are lowest for the 5% K_2O glass, peak for the 10% glass, and then decrease through the 15 and 20% compositions to a low in the 25% K_2O glass (Fig. 4). The SiO_5 content of pure silica glass is presumed to be very low, although there are only limited constraints on this: the most accurate upper bound is probably a detection limit of

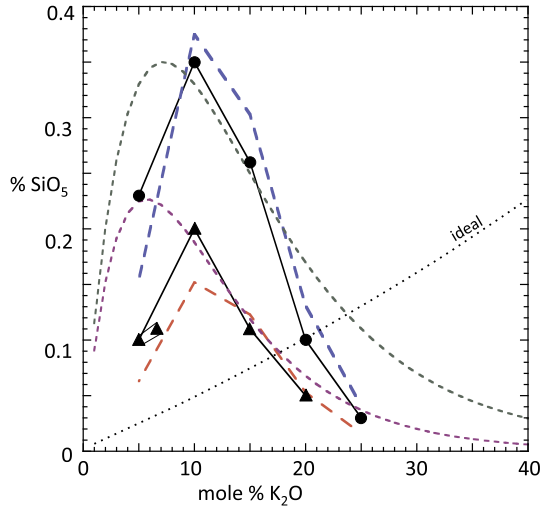

Fig. 4. Experimental data and model results for SiO_5 concentrations (mol % relative to total Si) as a function of composition and temperature in the K_2O-SiO_2 binary. Measured values (Table 1, with uncertainties) are shown by solid circles for FQ glasses and triangles for SC glasses, connected by solid lines for clarity. The elongated symbol for the 5% K2O, SC glass indicates estimated shift of glass composition due to partial crystallization of a silica phase. The experimental data have been extrapolated in temperature to predict isothermal values at 1000 K (blue, upper long-dashed segmented line) and 800 K (red, lower long-dashed segmented line), using estimated fictive temperatures and a constant ΔH_{app} for the speciation reaction described in the text. The black dotted line illustrates ideal solution behavior, adjusted to pass through the experimental point for the FQ 20% K_2O glass ($K_{app} = 0.0045$). The smooth curves with short dashes show predicted values at these two temperatures using a simple regular solution model for activities of non-bridging oxygens, with W = 60 kJ/mol and ΔH^0 for reaction (1) of 66.8 kJ/mol, and $K_{EQ} = 9.72 \times 10^{-5}$ at 1000 K chosen to give a curve maximum near to the experimental maximum. (For interpretation of the references to colour in this figure legend, the reader is referred to the web version of this article.)

0.3% from NMR studies of a ^{29}Si-enriched SiO_2 glass quenched from a melt at 6 GPa [9]. Extrapolating this limit down in pressure, based on results for $K_2Si_4O_9$ glass [17] suggests a 1 bar value in pure silica of $< < 0.1\%$, but more direct measurements would obviously be helpful.

Given the non-detection of SiO_5 and SiO_6 groups in pure, high-pressure silica, and observed lower contents of these species in $Na_2Si_2O_5$ glass (33% Na_2O) relative to $Na_2Si_4O_9$ glass (20% Na_2O) at a given run pressure, early studies pointed out that a maximum in the abundance of high coordinated silicon vs. silica content was likely [7,9], and discussed the possibility that the $K_2Si_4O_9$ composition (20% M_2O) was especially prone to the formation of such species. The formation of the wadeite polymorph of crystalline $K_2Si_4O_9$ (with 3 SiO_4 and 1 SiO_6 sites) at a relatively low pressure of about 2 GPa, as well as its possible energetic stability even at ambient pressure [56] also pointed towards this possibility. Our new data confirm that there is such a maximum, but that it is located at higher silica content than the previously-explored compositional range.

As in most studies of effects of composition on glass structure, elucidation of underlying chemical controls can be confounded by effects of temperature, if fictive temperatures (T_f) of the glasses in a series also vary substantially – which is generally the case. If data are obtained on the temperature effects themselves, structures of each composition can be corrected back to a constant fictive temperature, as has been done in several recent studies of boron coordination in borates and borosilicates [57,58]. In the present study, SiO_5 concentrations clearly depend strongly on cooling rate and thus on T_f. Furthermore, T_g, and thus T_f for a given cooling rate, is known to vary considerably with silica content [59,60]. If an isothermal plot of speciation vs. composition is the goal, then it is important to correctly define the equilibrium that controls this aspect of the structure. This can be done using a well-explored interaction of network cation species with oxygen ion species in oxide glasses and liquids.

Analogies to alkali borate and germanate glasses [61], in situ Raman spectroscopy on silicates [62,63], and other evidence has long suggested a reaction mechanism in which formation of higher-coordinated network species may be balanced by the conversion of NBO to BO, possibly connecting SiO_4 and SiO_5 groups [9]. This can be expressed as a reaction,

$$SiO_4 + NBO = SiO_5 \quad (1)$$

The mass and charge balance of this reaction can be confirmed if it is re-written in terms of oxygen species, where subscript denominators mark cation coordination number [42]:

$$4[O\text{–}Si_{1/4}Si_{1/4}]^0 + [O\text{–}Si_{1/4}]^{1-} = 5[O\text{–}Si_{1/4}Si_{1/5}]^{1/5-} \quad (2)$$

Charged species are necessarily balanced by modifier cations. Although these are not explicitly shown, their charge and size may certainly affect the extent of reaction.

The importance of the presence of NBO to network cation coordination increases is reflected in the non-detectability of high-coordinated Si in silica glass samples recovered from high pressures. It is further illustrated by the relatively rapid rate of formation of high-coordinated Al species (AlO_5 and AlO_6 groups) in NBO-rich alkali aluminosilicate compositions compared to 'fully polymerized' compositions such as $NaAlSi_2O_6$ and $NaAlSi_3O_8$. In the latter, mole fractions of alkali oxide and Al_2O_3 are equal, leading to low NBO contents [16,64]. Direct NMR measurements of changes in proportions of high coordinated Si, Al, and B as well as proportions of bridging and non-bridging oxygens for a few high pressure (3 to 12 GPa) silicate, aluminosilicate, and borosilicate glasses all confirm that this mechanism is a good description for NBO-rich compositions [13,65–68]. In compositions with inherently low NBO (e.g. pure SiO_2) or at pressures where NBO have been converted to BO connected to high-coordinated Si, other reactions will be important [69], most likely the formation of oxygen sites shared by three SiO_5 or SiO_6 groups, as in the transition from cristobalite to stishovite. The former structure has all SiO_4 and two-coordinated O, the latter all SiO_6 and three-coordinated O.

Reaction (1) can also be considered as a chemical equilibrium among species. In this case, an "apparent" equilibrium constant can be defined based on measurable mole fractions instead of thermodynamic activities, with.

$$K_{app} = X_{SiO5}/[(X_{SiO4})(X_{NBO})] \quad (3)$$

As has been done in a number of studies of the analogous equilibria among oxygen species and BO_3 and BO_4 groups in borates and borosilicates [58,70–74], the effect of temperature (or of fictive temperature) on speciation can then be characterized by an apparent standard state enthalpy change for reactions such as (1), which can be expressed in the integrated form of the van't Hoff equation [75]:

$$\Delta H_{app} = -2.303R(\log K_{app,T2} - \log K_{app,T1})/(1/T_2 - 1/T_1) \quad (4)$$

Here, the activity coefficients (or at least their products or ratios) are taken as independent of temperature. As noted below, these approximations are only a starting point, useful for the relatively small adjustments from experimental results to an isothermal plot. X_{SiO4} and X_{SiO5} are relative to total moles of Si; X_{NBO} is relative to total moles of O, although the molar basis will cancel out in the ΔH calculation. At the low concentrations of SiO_5 in these samples, $X_{SiO4} \approx 1$ and X_{NBO} can be calculated directly for each composition and is independent of temperature, with $X_{NBO} = 2X_{K2O}/(2 - X_{K2O})$.

To apply this approach to estimating ΔH_{app} values from the present data set on SiO_5 concentrations, fictive temperatures for fast-quenched (FQ) and slowly-cooled (SC) samples must first be estimated. Unlike in some previous studies, small sample sizes here did not allow ready

measurement of either T_f or T_g by differential scanning calorimetry [72]. Useful estimates can, however, be obtained by assuming that T_f for the SC glasses are the same as T_g values reported in the literature for annealed samples of these compositions [59,60]. T_f for the FQ glasses can then be estimated from the differences in the cooling rates known for the SC and estimated for the FQ samples, using the well-known method of Moynihan [71,76] and approximating the activation energy for viscosity near to T_g as a constant of 460 kJ/mol, based on $K_2Si_4O_9$ [77] (Table 1). With uncertainties in cooling rates and SiO_5 contents, derived values of ΔH_{app} have large error bars, but are all about 20 to 35 kJ/mol, consistent with previous estimates [10]. Given the partial crystallization of the 5% K_2O glass, estimation of ΔH_{app} is especially uncertain and is not tabulated. Based on the measured SiO_5 content for the FQ samples, the estimated T_f, and, for consistency a constant value for ΔH_{app} of 30 kJ/mol, the speciations at fixed temperatures of 1000 and 800 K were calculated and plotted in Fig. 4. The overall pattern of an obvious maximum near to 10% K_2O remains.

As noted in Section 3.4 below, a non-ideal solution model treatment for the thermodynamic activity of NBO predicts that ΔH_{app} should vary systematically with composition, even with a constant "true" ΔH^0 for reaction (1). These predicted values for one such model are also listed in Table 1, based on a starting value for ΔH_{app} at the 20% K_2O composition of 30 kJ/mol. Applying these values to extrapolate experimental data to 1000 K and 800 K isotherms would have only a minor effect on the plot in Fig. 1, moving the 800 K points for the lower K_2O compositions upwards.

3.4. Thermodynamic analysis of SiO_5 variation with composition

At the low concentrations of SiO_5 in these samples, X_{NBO} is approximately a function of composition only, scaling directly with the mole fraction of K_2O as noted above. Given that $X_{SiO4} \approx 1$, an "ideal" solution for the binary would suggest that the apparent equilibrium constant for reaction (1) should actually be constant, and that X_{SiO5} should thus also increase monotonically (although not linearly) with K_2O content, i.e.:

$$X_{SiO5} \approx K_{app}\,(X_{NBO}) \tag{5}$$

$$\approx K_{app}\,[2X_{K2O}/(2-X_{K2O})]$$

The shape of the experimental, and of the estimated isothermal curves in Fig. 4 show that this is clearly far from the case, i.e. that the true equilibrium constant K_{EQ} cannot be equivalent to K_{app}. Such non-ideal behavior is also suggested by variations with composition in the analogous ΔH_{app} values estimated from T_f effects on BO_3-BO_4 speciation in borosilicates [72].

This result leads to the question of what modification of the ideal solution approximation for NBO activity might provide a better match to the observed SiO_5 variations. The most common approach to parameterizing non-ideality is the "regular solution" model, in which a non-zero enthalpy of mixing is introduced that is parabolic with composition. A single energetic interaction parameter, W, is included, which results in a compositional dependence of activity coefficients, γ, for each of two (or more) components that mix in the solution [78]:

$$\log\,\gamma_1 = (1-X_1)^2\,[W/(2.303RT)] \tag{6}$$

Here, X_1 is the mole fraction of component 1, the thermodynamic activity of which is simply $a_1 = \gamma_1\,X_1$. $W = 0$ and $\gamma = 1$ in an ideal solution. A positive value of W reflects a lower energy for like-like pairs of component species compared to unlike pairs (i.e. clustering vs. mixing), and may be correlated with physical unmixing (phase separation).

Again given the low concentrations of SiO_5 species in the glasses studied here, and the much higher concentrations of NBO, the initial focus of a non-ideal modification to Eq. (3) should probably be on the mixing behavior, and thermodynamic activity, of the non-bridging oxygen species: ideal solution behavior is often the best approximation for mixing of dilute components such as SiO_5. Thus considering variation from ideal mixing only for the oxygen species, taken here as simply NBO and BO, Eq. (3) could thus be re-written as:

$$K_{EQ} = X_{SiO5}/[(X_{SiO4})\,(\gamma_{NBO}\,X_{NBO})] \tag{7}$$

$$\log\,(\gamma_{NBO}) = (1-X_{NBO})^2\,[(W/2.303RT)] \tag{8}$$

X_{SiO5} can then be modeled by choosing composition-independent values of K_{EQ} and W that yield an SiO_5 concentration consistent with experiment at a single T_f and X_{K2O}, and the variation in speciation predicted as a function of composition. The effect of temperature can be introduced as above, with a fixed standard state ΔH^0, which now will be independent of composition and chosen for consistency with experiment. The value of ΔH^0 will be different from ΔH_{app}: because of the inverse effect of T on γ_{NBO} in this model, ΔH^0 will be larger than ΔH_{app} for $W > 0$. ΔH^0 is related to the variation in K_{EQ} with temperature as ΔH_{app} is related to the variation of K_{app} with T (Eq. (4)). For example, for $\Delta H_{app} = 30$ kJ/mol as used above, and $W = 60$ kJ/mol as estimated below, a value of ΔH^0 of 66.8 kJ/mol gives the same variation in speciation with temperature.

The theoretical shapes of the curve predicted for SiO_5 concentration for a wide range of positive values of W are compared in Fig. 5, for 1000 K and a maximum species concentration near that of the observed maximum. For W near to 0 the curve has the expected direct, monotonic dependence on X_{K2O}. For a value of $W = 20$ kJ/mol the predicted curve reaches a maximum and remains nearly constant over the compositional range shown; for higher values of W a rapid initial increase with X_{K2O} is followed by a maximum and a less steep decrease at higher alkali contents. At higher X_{K2O} above the range plotted, these curves may show physically unrealistic inflections. None of the curves predicted with this simple one-parameter adjustment of the ideal solution model matches the experimental data (adjusted to the corresponding isotherms) exactly, but $W \approx 60$ kJ/mol may give the closest approximation as shown in Fig. 4, given large uncertainties in data and extrapolations in temperature. As in many applications of this type of model to liquid or solid solutions, for example to match the liquidus curves in alkali silicate binaries [51], additional parameters could be introduced (making W a function of X and/or T), or different components chosen, to adjust the shape of the predicted curve. Given the novelty and uncertainties in the results, this fitting exercise is not undertaken here. Instead, the purpose of this rough thermodynamic approximation is to illustrate possible qualitative relationships among

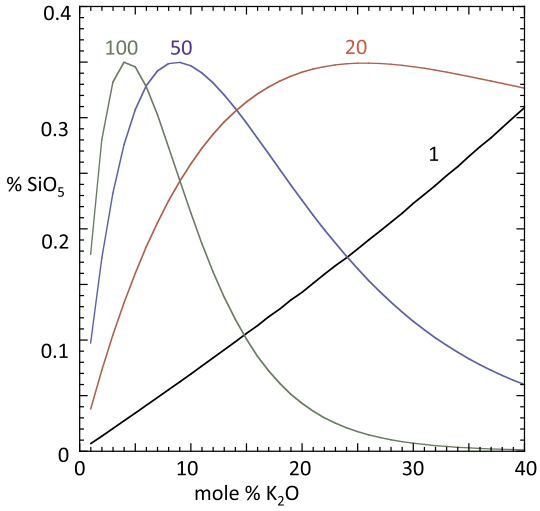

Fig. 5. Modeled SiO_5 concentrations (mol % relative to total Si) at 1000 K for W = 100, 50, 20, and 1 kJ/mol (left to right, as labeled) to illustrate the wide range of possible curve shapes. The last of these is close to an "ideal" solution.

energetic interactions between different oxygen anionic species, network cation coordination, and likely effects on melt and glass properties.

In this model, the highly non-linear shape of the predicted SiO_5 curve is a response to an initial steep increase in the activity of NBO with increasing X_{K2O} and initially high values of γ_{NBO} (high excess enthalpy and free energy of mixing for the NBO at low concentrations), promoting the formation of SiO_5 via reaction (1). This is followed by a decrease in SiO_5 as γ_{NBO} becomes less predominant according to Eq. (8), even though X_{NBO} continues to rise with increasing X_{K2O}. The simple, parabolic heat of mixing in a one-parameter regular solution model is likely to be a great oversimplification of energetic consequences of melt structure, but the *form* of the NBO activity variation with composition does reflect the expected tendency of NBO to cluster together for more effective local charge compensation by available modifier cations: isolated NBO are energetically relatively unfavorable, especially when the modifier cation is large and monovalent, requiring a high coordination number of its own. Charge balance of an isolated NBO by one such cation would result in significant underbonding; correspondingly for the cation, a single NBO in its first coordination shell would provide a highly asymmetrical, probably relatively high-energy, environment.

This tendency to cluster can of course be the precursor to physical liquid-liquid unmixing, as is well known in binary silicate solutions in systems with alkaline earth oxides, and with Li_2O and Na_2O, and which is predicted at sub-T_g temperatures in the K_2O-SiO_2 system [50,51]. It has also been long explored in terms of the "modified random network model", especially in relation to ionic transport in interconnected percolation domains [79]. As modifier oxide content increases, there is less drive for clustering as both cation and anion local charge balance becomes more favorable. For example, in the low-pressure (all SiO_4) crystalline phase of $K_2Si_4O_9$ (20% K_2O), each NBO is coordinated by 3 K^+, and each K^+ has two or three NBO (plus several BO) in its first shell [80], without the need for a non-homogeneous distribution of cations. Equilibria such as that expressed in reaction (1) (and corresponding reactions for borate and germanate systems as discussed below) are thus shifted back to the lower coordination, left-hand side in high-modifier compositions. These effects are captured to some degree by the highly non-linear dependence of the activity coefficient for NBO on composition as described by the regular solution approximation in Eq. (8).

It is also important to note that the model described here for NBO activities and SiO_5 concentrations is not intended to be a complete thermodynamic description of this system, as it does not account for other interactions among either anionic or cationic species that affect the overall free energy of the solution. This can be seen in the fact that in a more standard regular solution model, typically designed to describe all effects of composition on the free energy of mixing, the critical temperature of unmixing (the top of the solvus) is predicted as W/2R, which would be about 3600 K for W = 60 kJ/mol, in contrast to the estimated value of about 830 K for the K_2O-SiO_2 system based on extrapolation of observations in ternary alkali silicate systems [50,51]. The simple approach here is also somewhat unrealistic physically, as non-ideality of mixing of oxygen species could well be correlated to non-ideality in mixing of cationic species. For example, if SiO_5-SiO_5 pairs are considered to be energetically unfavorable for reasons of an underbonded oxygen linkage (as has long been suggested for BO_4-BO_4 pairs in alkali borate glasses [58,105]), non-ideality in mixing of SiO_4 and SiO_5 could be introduced into Eq. (7) that could contribute to the observed speciation. However, unlike BO_4 groups in alkali borate systems (Section 3.7, below), SiO_5 species remain at very low concentrations at 1 bar pressures, suggesting that interactions will be limited and contributions to overall mixing energetics relatively small. A physical correlation between oxygen species mixing and silicate species mixing could indeed be expected if NBO are more likely to occur on network species with lower cation coordination, again in parallel to what is expected in borate systems.

3.5. Other compositional effects on SiO_5 concentrations

Early studies of SiO_5 in both ambient and high pressure glasses reported concentrations for Na tetrasilicate compositions (20% Na_2O) that were somewhat lower than for $K_2Si_4O_9$ glass [9,11], and explanations were suggested in terms of modifier cation field strength and the difficulty of NBO charge balancing by larger modifier cations in high silica compositions. In ^{29}Si-enriched, ambient pressure $MgSiO_3$ and $CaSiO_3$ glasses, no SiO_5 was detectable, although this species has been observed in high pressure $CaSi_2O_5$ and $MgSiO_3$ glasses [12,14]. In the new results here, the lack of detectable SiO_5 in 20% and 33% Li_2O glasses may be related to such a field strength trend, but may also be a consequence of the strongly non-linear shape to the SiO_5 vs. composition curve. The 20% Li_2O glass is clearly phase separated at the sub-optical scale [44], likely resulting in regions of very high SiO_2 content and regions of much lower silica content, the latter probably close to the 33% composition. These two compositional domains may lie on opposite sides of a SiO_5 maximum in this binary, bringing the concentration of this species to levels below detection in both. For Ca, and Mg silicate binaries at low pressures, liquid-liquid phase separation may also prevent the formation of single-phase glasses at high enough silica contents to produce measurable SiO_5 concentrations; in Na-silicates single phase glasses may also be restricted to compositions with > 15 to 20% modifier oxide.

3.6. SiO_5 and silicate melt properties

At the low concentrations reported here for SiO_5 (< 0.5%), this species, and its variation with composition and temperature, is unlikely to have important consequences for models of bulk thermodynamic properties such as density, heat of formation, or configurational entropy or heat capacity [75], especially at low temperatures near to T_g, apart from the implications discussed above for the activities of major components such as NBO. However, since some of the earliest classical molecular dynamics (MD) simulations of oxide liquid structure and dynamics, this species has been suggested as a possible "transition complex" in the swapping of network bonds that probably controls network component diffusion and viscosity, at least for high silica contents [18,81]. This mechanistic role has been explored in detail in recent theoretical studies [26–33]. Improved experimental determinations of low concentration, but dynamically critical, species should thus

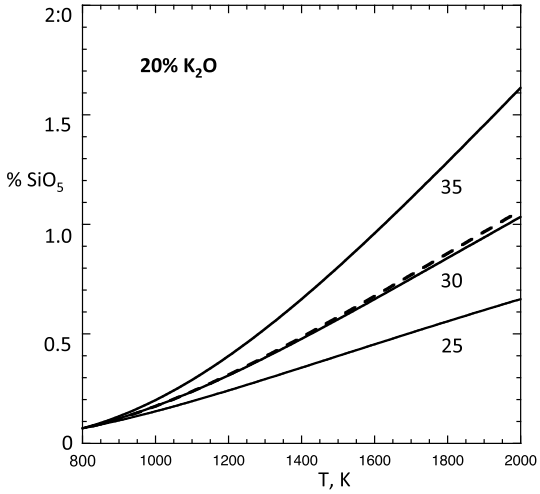

Fig. 6. Effect of temperature on SiO_5 concentration for 20% K_2O liquid, calculated for the ideal solution case and ΔH_{app} = 35, 30, and 25 kJ/mol (upper to lower solid curves), as well as for the non-ideal solution case with W = 60 kJ/mol and ΔH^0 = 66.8 kJ/mol (dashed curve). The low temperature starting points are chosen to match the non-ideal curve in Fig. 4 for this composition.

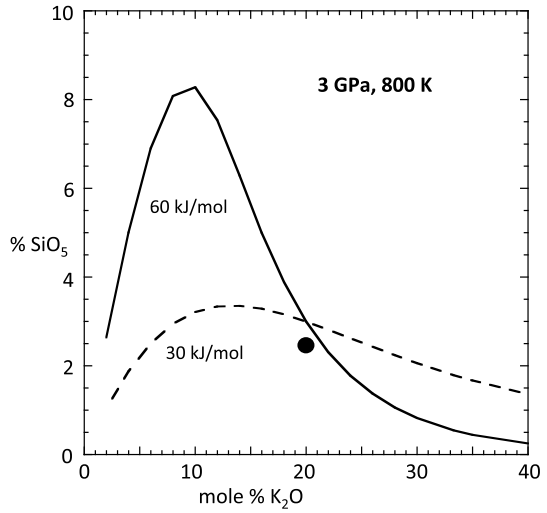

Fig. 7. Possible effects of composition in SiO_5 concentrations in metastable K_2O-SiO_2 liquids at 800 K and 3 GPa, based on a recent measurement for a 20% K_2O glass quenched from this pressure and 743 K (solid circle [17]) and W = 60 kJ/mol, which roughly matches the compositional dependence at 1 bar (Fig. 4). As pressure may have as-yet unknown effects on W, a curve is also shown for W = 30 kJ/mol.

be important in validating such models and their predictions of both thermodynamic and transport properties. It is important to note that although extrapolation of the results given here to much higher temperatures has large uncertainties, maximum SiO_5 contents may exceed 1% at 2000 K, a typical 'low' temperature for fully relaxed MD simulations of silicate liquids (Fig. 6). Such concentrations may be high enough to be modeled with some accuracy by large classical MD models, which generally treat 1000's of ions, and even possibly advanced ab initio MD.

It is at higher pressures where SiO_5 (and SiO_6) species must begin to be important for bulk melt properties, as the denser oxygen packing resulting from increased cation coordination numbers is favored. Early experimental and theoretical studies of silicate and aluminosilicate melts, for example, suggested that anomalous decreases in viscosity with pressure could be the result of such structural changes [18,82]. Our recent results provide new data on $K_2Si_4O_9$ (20% K_2O), which show that SiO_5 contents may be considerably higher than expected from previous data because of technical issues involving transient pressure drops from high initial run temperatures, e.g. 2.4% SiO_5 near to T_g at 3 GPa [17], compared to 0.05% at 1 bar. The strong non-linearity with composition in SiO_5 concentrations seen here for ambient pressure glasses is expected to also play a role at high pressure where these species are much more abundant, although mixing properties such as regular solution interaction parameters may well be pressure-dependent also. Similar effects for SiO_6 might also be expected. We currently have very few constraints on such compositional effects at pressure: a hypothetical prediction at 800 K and 3 GPa, based on recent data for $K_2Si_4O_9$ is shown in Fig. 7 for W = 60 kJ/mol and for W = 30 kJ/mol.

It is not the purpose of this contribution to try to predict high pressure silicate melt properties in detail, but it is useful to note analogies between such liquids and other systems better known from 1 bar experiments. In ambient pressure silicate liquids, molar volumes (gram formula weight divided by density) are generally close to linear functions of composition, and can thus be predicted with good accuracy by models with constant partial molar volumes, usually modeled for convenience as those of the simple oxide components [38]. Most relevant here is the finding of a constant partial molar volume for SiO_2 that corresponds to the approximation that all silica, the predominant chemical component, is in a fixed, tetrahedral coordination of Si. Such models have been extended to moderate pressures (a few GPa) by inclusion of partial molar compressibilities for the same, fixed oxide components [83].

In marked contrast are the behaviors of other simple glass forming oxide systems. As illustrated in a recent review [42], for example, molar volumes as functions of composition in alkali borate glasses and melts, and in alkali germanate glasses and melts may be highly non-linear with composition, probably in large part because of well-known initial increases, maxima, then decreases in network cation coordination as alkali oxide is added to the pure network former, i.e. BO_3 to BO_4 to BO_3, and GeO_4 to GeO_5 (+ GeO_6?) to GeO_4 speciation. Models of such data can be complex to account for structural details, but at very least must assume that partial molar volumes of the network oxide components change significantly with composition as coordination numbers shift. In the case of silicate melts at pressures high enough for SiO_5 (and SiO_6) to begin to be major components (perhaps above ca. 20 GPa, representing most of the Earth's mantle), such non-linearity in composition must be expected. For example, the known dramatic difference between the molar volumes of crystalline silica with SiO_4 groups (25.7 cm^3/mol for cristobalite at 298 K and 1 bar) vs. SiO_6 groups (14.0 cm^3/mol for stishovite) should be reflected in liquid partial molar volumes of such components. If their proportions vary in the highly non-linear fashion as demonstrated here for the K_2O-SiO_2 binary, predictive models of melt (and glass) properties will have to be correspondingly complex, especially at higher silica contents. Of course, at pressures where all Si is in SiO_6 groups, compositional variation of volume may return to greater simplicity. The need for such structurally realistic thermodynamic models for silicates at high pressures has been recognized in a sophisticated development of their form and implications for equations of state [84], but as yet the required structural constraints are largely taken from computer simulations [85].

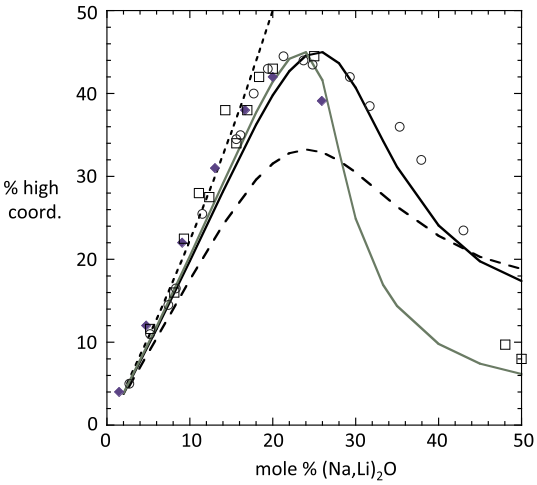

Fig. 8. Model calculations for mole % BO_4 (out of total B) vs. mole % of alkali oxide in M_2O–$BO_{3/2}$ binaries, the latter component chosen for more direct comparison with silicate and germanate systems instead of the more conventional B_2O_3. Note the roughly 100× difference in vertical scale relative to plot for SiO_5 at 1 bar in Fig. 4. Uppermost to lowermost curves are calculated for no NBO (short dashed line); model with W = 30 kJ/mol at 800 K (solid black line); with W = 30 kJ/mol at 1000 K (long dashed line); and with W = 40 kJ/mol at 800 K (solid green line). The T effect is based on an estimated ΔH_{app} for reaction (9) of −30 kJ/mol for a composition near the curve maximum. Also shown are experimental data for Na borate glasses by high-field MAS NMR (blue diamonds) [106]), for Na borate glasses by low-field 'wideline' NMR (small open squares) [107], and for Li borate glasses (small open circles) [108]. See original publications for estimated uncertainties on experimental data points. (For interpretation of the references to colour in this figure legend, the reader is referred to the web version of this article.)

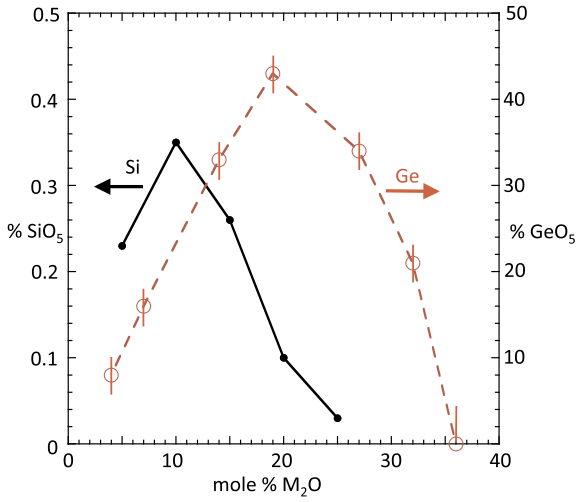

Fig. 9. Experimental data for SiO_5 in fast-quenched K-silicate glasses (black solid circles and line, left side scale) compared with one estimate for high-coordinated Ge (taken for simplicity here as all GeO_5), based on ^{17}O NMR (red open circles and dashed line, right side scale) [93]. Note 100× larger concentration scale for the latter. (For interpretation of the references to colour in this figure legend, the reader is referred to the web version of this article.)

3.7. Analogous behavior of alkali silicate, borate and germanate systems?

In the previous section, contrasting patterns were noted for the bulk property behavior between alkali silicates, with > 99% SiO_4 at ambient pressure, and alkali borates and germanates, with roughly equal concentrations of two or even three network cation coordinations at some point in their binaries. However, the *shape* of the SiO_5 vs. X_{K2O} curve in Fig. 4 does have a striking similarity to those of plots of BO_4 content when the latter are presented vs. mole fraction of alkali oxide (M_2O) relative to $M_2O + BO_{3/2}$ rather than the more conventional "R" axis (molar ratio M_2O/B_2O_3). On the former basis, the well-known maximum at R ≈ 0.5 is equivalent to a maximum at $X_{M2O} \approx 0.2$. Several early and recent sets of NMR data for boron coordination are plotted on this basis in Fig. 8. Germanium cation coordinations are less well known than those for boron, and there is considerable variation in both experimental findings from X-ray and neutron scattering [86,87], Raman [88–90] and NMR spectroscopies [91–93] and in interpretations of results. Nonetheless, maxima in Ge coordination numbers in alkali germanate systems have most commonly been indicated near to 15 to 20 mol% M_2O. One estimate based on recent ^{17}O NMR data [93] (choosing GeO_5 as the only high coordinated species for simplicity) is compared with the new data for ambient pressure SiO_5 in Fig. 9, scaled by a factor of 100 to account for the large differences in absolute concentrations. As is most commonly the case, neither the borate nor the germanate data have been corrected for systematic variations in T_g and hence in T_f across the binaries, but this is not expected to have a large effect on the overall curve shapes [58].

As noted above, reactions in which network cations with low coordination are converted to higher coordination through the conversion of NBO to BO (reaction (1) for silicates) have long been suggested as important in borate and germanate systems; indeed the direct measurement of NBO concentrations by ^{17}O NMR has been useful for estimating Ge speciation [93,94]. It thus becomes interesting to consider the effects of a simple variation from non-ideal mixing of oxygen ion species as explored above for the potassium silicate system, taking speciation reactions as analogous to reaction (1):

$$BO_3 + NBO = BO_4 \quad (9)$$

$$GeO_4 + NBO = GeO_5 \quad (10)$$

An analogous reaction to form GeO_6 groups can be written with the "consumption" of two NBO. As above, the mass and charge balance of these can be confirmed by writing in terms of oxygen speciation:

$$3[O\text{–}B_{1/3}B_{1/3}]^0 + [O\text{–}B_{1/3}]^{1-} = 4[O\text{–}B_{1/3}\,B_{1/4}]^{1/4-} \quad (11)$$

$$4[O\text{–}Ge_{1/4}Ge_{1/4}]^0 + [O\text{–}Ge_{1/4}]^{1-} = 5[O\text{–}Ge_{1/4}Ge_{1/5}]^{1/5-} \quad (12)$$

In some ways the silicate and borate or germanate systems are very different, of course, at least at low pressure: K_{app} and K_{EQ} for these reactions in the borate and germanate binaries are several orders of magnitude higher than for the silicate system. The high coordinated states are energetically much more stable in the former, given the smaller radius of B^{3+} (favoring BO_3 formation but ease of transition to BO_4) and the larger radius of Ge^{4+} relative to Si^{4+} (favoring GeO_5 and GeO_6 formation). In other terms, the standard state free energy changes for reactions (9) and (10) ($-2.303RT \log K_{EQ}$), although still positive (since $K_{EQ} < 1$), are much smaller than for the silicate system. Also in contrast with the silicates, for the borates the enthalpy change (either ΔH_{app} calculated as above from measured concentrations or a constant ΔH^0 in a more complete thermodynamic treatment) for reaction (9) has long been known to be negative instead of positive [58,73,95], as the left hand side is favored at higher temperatures instead of the right side. The effect of temperature on germanium coordination in alkali germanate liquids has apparently not been determined. However, in both alkali borate and germanates, non-linearities with composition in molar volumes are qualitatively similar in glasses and liquids, indicating that elevated temperatures do not fundamentally change effects on network cation coordination [39].

In spite of these differences, the simple regular solution model developed above for NBO/BO mixing in alkali silicates can be explored for the better-known alkali borates. Here, the calculation of speciation must be done iteratively, as NBO content cannot be approximated from composition alone but is closely tied to the relatively high concentrations of both BO_3 and BO_4 through reaction (9). As for the silicates, a wide range of curve shapes can be derived, depending on the magnitude of the single interaction parameter W. However, a value of W = 30 kJ/mol, combined with a value of K_{EQ} to roughly match the BO_4 maximum value at 800 K, yields a curve that strongly resembles the well-known experimental shape. This is especially true as the temperature of the calculation is adjusted downwards to values near to empirical T_g's (about 700 to 800 K), where, at low X_{M2O}, reaction (9) goes nearly to completion and NBO contents are minimized. At higher temperatures, more NBO remain and BO_4 contents are lower, as was clearly seen in early, more complete statistical thermodynamic modeling of the system [96]. ΔH_{app} data for alkali borates are actually not very well constrained, as most fictive temperature experiments have been done on borosilicates. The 1000 K curve in Fig. 8 is calculated using a value of −30 kJ/mol for a composition near the maximum. As for the SiO_5 calculations shown in Table 1, the model (W = 30 kJ/mol) yields ΔH_{app} values for the borate reaction that vary with composition, increasing in magnitude from about −26 kJ/mol at 5% M_2O (on an M_2O-$BO_{3/2}$ molar basis) to −32 kJ/mol at 25% M_2O. This is the same trend with composition as estimated from in situ Raman spectroscopy on Na borate liquids [97], although in that study the apparent range (with large uncertainties) was from about −20 to −60 kJ. Note that the highest Na_2O concentration in that study (33%) corresponds to 20% on the $BO_{3/2}$ molar basis used here to facilitate comparisons among silicates, borates and germanates.

This pattern of variation in boron coordination with composition in alkali borate glasses has been known since some of the earliest applications of solid-state NMR spectroscopy in the late 1950's and early 1960's [98–100]. Data have continually improved with the development of high-field, high resolution methods (e.g. [101,102]). Observed boron coordination variation has long been modeled in terms of mixtures of "superstructural units" based originally on corresponding crystal structures, using either strictly empirical formulations of their proportions (e.g. [103]) or more sophisticated thermodynamic models

of "associated solutions" [41,104]. Other recent work has considered primarily the short-range connections among three- and four-coordinated borate groups in constraining network topology and hence dynamical properties [105]. The structural richness of these models can allow prediction or parameterization of speciation much more precisely than the approach taken here, which is not meant to capture a complete picture of either the structure or the governing thermodynamics. In particular, the long-suggested 'avoidance' of BO_4-BO_4 pairs, because of energetically unfavorable underbonding on the bridging oxygen, is likely to be quite important and would introduce substantial non-ideality of mixing in a more complete thermodynamic formuation. Nonetheless, the observation that the pattern of silicon coordination changes with composition at very low concentrations of SiO_5 (and perhaps at high concentrations at high pressure) seems to parallel the patterns for high coordinated B in borates (and for Ge in germanates), and that a single type of network speciation reaction with a minimum number of adjustable parameters (three, if temperature effects are included) predicts curves that strongly resemble experiment, is intriguing and indicates an underlying commonality among oxide melt systems that may not have been previously appreciated. Just as structure/property relationships in germanate and borate crystals and glasses have been used at times to help predict how silicates might behave at high pressures, detailed data on silicate speciation even at ambient pressure may provide new insights into compositional effects on network cation coordination in germanates and borates.

4. Conclusions

Using isotopically enriched ^{29}Si, concentrations of SiO_5 groups can be readily measured in ambient pressure alkali silicate glasses down to levels of about 0.02 molar percent. SiO_5 varies systematically and highly non-linearly with composition from low to high modifier contents in the potassium silicate binary, reaching a maximum at about 10% K_2O. This species is below detection limit in lithium silicates, however. Higher fictive temperatures result in higher concentrations. The predominant mechanism of formation of SiO_5 probably involves the conversion of non-bridging oxygens to bridging oxygens linking SiO_4 tetrahedra to higher coordinate species. If this is the case, then the observed compositional variation can be at least roughly approximated by a simple thermodynamic model involving non-ideal mixing of bridging and non-bridging oxygens, with a single positive interaction parameter that is consistent with known tendencies for modifier clustering and phase separation. Long-known patterns of network cation coordination variation with composition in alkali borates and germanates, although involving about 100 times greater concentrations of higher coordinated species (BO_4 and GeO_5/GeO_6), are qualitatively similar to these new observations for silicates, suggesting an underlying commonality in the energetics of mixing of oxygen species. Well-known non-linearities in chemical and physical properties in borate and germanate systems thus suggest that in silicates at pressures where SiO_4, SiO_5 (and SiO_6) groups all have high concentrations, compositional effects on properties are likely also to be complex, requiring considerable new experimental and theoretical efforts to accurately constrain models.

Acknowledgments

This research was supported by the U.S. National Science Foundation, grant numbers EAR-1521055 and DMR-1505185. We thank an anonymous reviewer for helpful comments, especially about the possible role of non-ideal mixing of cationic species, and to the editors of this special issue of JNCS.

References

[1] B.G. Aitkin, R.E. Youngman, Borophosphosilicate glasses: properties and structure, Phys. Chem. Glasses 47 (2006) 381.
[2] M. Nogami, K. Miyamura, Y. Kawasaki, Y. Abe, Six-coordinated silicon in SrO-P_2O_5-SiO_2 glasses, J. Non-Cryst. Solids 211 (1997) 208.
[3] R. Dupree, D. Holland, M.G. Mortuza, Six-coordinated silicon in glasses, Nature 328 (1987) 416.
[4] R. Dupree, D. Holland, M.G. Mortuza, J.A. Collins, M.W.G. Lockyer, Magic angle spinning NMR of alkali phospho-alumino-silicate glasses, J. Non-Cryst. Solids 112 (1989) 111.
[5] M.G. Mortuza, M.R. Ahsan, J.A. Chudek, G. Hunter, First evidence for the coexistence of four-, five- and six-coordinated silicon in glasses prepared at ambient pressure, Chem. Comm. (2000) (2000) 2055.
[6] L. van Wüllen, B. Gee, L. Zuchner, M. Bertmer, H. Eckert, Connectivities and cation distributions in oxide glasses: new results from solid-state NMR, Ber. Bunsen-Gesell, Phys. Chem. 100 (1996) 1539.
[7] J.F. Stebbins, P. McMillan, Five- and six- coordinated Si in $K_2Si_4O_9$ glass quenched from 1.9 GPa and 1200°C, Am. Mineral. 74 (1989) 965.
[8] X. Xue, J.F. Stebbins, M. Kanzaki, R.G. Tronnes, Silicon coordination and speciation changes in a silicate liquid at high pressures, Science 245 (1989) 962.
[9] X. Xue, J.F. Stebbins, M. Kanzaki, P.F. McMillan, B. Poe, Pressure-induced silicon coordination and tetrahedral structural changes in alkali silicate melts up to 12 GPa: NMR, Raman, and infrared spectroscopy, Am. Mineral. 76 (1991) 8.
[10] J.F. Stebbins, Experimental confirmation of five-coordinated silicon in a silicate glass at 1 atmosphere pressure, Nature 351 (1991) 638.
[11] J.F. Stebbins, P. McMillan, Compositional and temperature effects on five coordinated silicon in ambient pressure silicate glasses, J. Non-Cryst. Solids 160 (1993) 116.
[12] J.F. Stebbins, B.T. Poe, Pentacoordinate silicon in high-pressure crystalline and glassy phases of calcium disilicate ($CaSi_2O_5$), Geophys. Res. Lett. 26 (1999) 2521.
[13] J.R. Allwardt, B.C. Schmidt, J.F. Stebbins, Structural mechanisms of compression and decompression in high pressure $K_2Si_4O_9$ glasses: an investigation utilizing Raman and NMR spectroscopy of high-pressure glasses and crystals, Chem. Geol. 213 (2004) 137.
[14] S.J. Gaudio, S. Sen, C.E. Lesher, Pressure-induced structural changes and densification of vitreous $MgSiO_3$, Geochim. Cosmochim. Acta (2008) 1222.
[15] K.E. Kelsey, J.F. Stebbins, J.L. Mosenfelder, P.D. Asimow, Simultaneous aluminum, silicon, and sodium coordination changes in 6 GPa sodium aluminosilicate glasses, Am. Mineral. 94 (2009) 1205.
[16] S. Bista, J.F. Stebbins, B. Hankins, T.W. Sisson, Aluminosilicate melts and glasses at 1 to 3 GPa: temperature and pressure effects on recovered structural and density changes, Am. Mineral. 100 (2015) 2298.
[17] J.F. Stebbins, S. Bista, Pentacoordinated and hexacoordinated silicon cations in a potassium silicate glass: effects of pressure and temperature, J. Non-Cryst. Solids 505 (2019) 234.
[18] C.A. Angell, P.A. Cheeseman, S. Tamaddon, Pressure enhancement of ion mobilities in liquid silicates from computer simulation studies to 800 kilobars, Science 218 (1982) 885.
[19] S. Brawer, Relaxation in Viscous Liquids and Glasses, American Ceramic Society, Inc, Columbus, 1985.
[20] S.B. Liu, J.F. Stebbins, E. Schneider, A. Pines, Diffusive motion in alkali silicate melts: an NMR study at high temperature, Geochim. Cosmochim. Acta 52 (1988) 527.
[21] I. Farnan, J.F. Stebbins, A high temperature ^{29}Si NMR investigation of solid and molten silicates, J. Am. Chem. Soc. 112 (1990) 32.
[22] B.T. Poe, P.F. McMillan, D.C. Rubie, S. Chakraborty, J. Yargar, J. Diefenbacher, Silicon and oxygen self-diffusivities in silicate liquids measured to 15 gigpascals and 2800 kelvin, Science 276 (1997) 1245.
[23] D.C. Rubie, C.R. Ross, M.R. Carroll, S.C. Elphick, Oxygen diffusion in $Na_2Si_4O_9$ liquid up to 10 GPa and estimation of high-pressure melt viscosities, Am. Mineral. 78 (1993) 574.
[24] D. Tinker, C.E. Lesher, G.M. Baxter, T. Uchida, Y. Wang, High-pressure viscometry of polymerized silicate melts and limitations of the Eyring equation, Am. Mineral. 89 (2004) 1701.
[25] P.F. McMillan, M.C. Wilding, High pressure effects on liquid viscosity and glass transition behaviour, polyamorphic phase transitions and structural properties of glasses and liquids, J. Non-Cryst. Solids 355 (2009) 722.
[26] X. Yuan, A.N. Cormack, Local structures of MD-modeled vitreous silica and sodium silicate glasses, J. Non-Cryst. Solids 283 (2001) 69.
[27] J. Machacek, O. Gedeon, M. Liska, Relaxation of structural units in MD simulated silicate glasses, Phys. Chem. Glasses 47 (2006) 266.
[28] J. Machacek, O. Gedeon, M. Liska, Molecular approach to the 5-coordinated silicon atoms in silicate glasses, Phys. Chem. Glasses 48 (2007) 345.
[29] I. Bakk, I. Deme, D. Szieberth, L. Nyulaszi, Molecular level investigation of the dynamic structure model in molten and solid alkali glasses, Struct. Chem. 23 (2012) 1729.
[30] R.H. Doremus, Viscosity of silica, J. Appl. Phys. 92 (2002) 7619.
[31] R.H. Doremus, Transport of oxygen in silicate glasses, J. Non-Cryst. Solids 349 (2004) 242.
[32] T. Ohkubo, E. Tsuchida, K. Deguchi, S. Ohki, T. Shimuzu, T. Otomo, Y. Iwadate, Insights from ab initio molecular dynamics simulations for a multicomponent oxide glass, J. Am. Ceram. Soc. 101 (2017) 1122.
[33] J. Cuny, Y. Xie, C.J. Pickard, A.A. Hassanali, Ab initio quality NMR parameters in solid-state materials using a high-dimensional neural-network representation, J. Chem. Theory Comput. 12 (2016) 765.
[34] J.D. Kubicki, A.C. Lasaga, Theoretical reaction pathways for the formation $[Si(OH)_5]^{1-}$ and the deprotonation of orthosilicic acid in basic solutions, Geochim. Cosmochim. Acta 57 (1993) 3847.

[35] B. Herreros, S.W. Carr, J. Klinowski, 5-coordinate Si compounds as intermediates in the synthesis of silicates in nonaqueous media, Science 263 (1994) 1585.
[36] S.D. Kinrade, J.W. Del Nin, A.S. Schach, T.A. Sloan, K.L. Wilson, C.T.G. Knight, Stable five- and six-coordinated silicate anions in aqueous solutions, Science 285 (1999) 1542.
[37] T. Fuss, C.S. Ray, N. Kitamura, M. Makihara, D.E. Day, Pressure induced nucleation in a Li_2O-$2SiO_2$ glass, J. Non-Cryst. Solids 318 (2003) 157.
[38] R.A. Lange, A revised model for the density and thermal expansivity of K_2O-Na_2O-CaO-MgO-Al_2O_3-SiO_2 liquids from 700 to 1900 K: extension to crystal magmatic temperatures, Contrib. Mineral. Petrol. 130 (1997) 1.
[39] E.F. Riebling, Structural similarities between a glass and its melt, J. Am. Ceram. Soc. 51 (1968) 143.
[40] A.K. Varshneya, Fundamentals of Inorganic Glasses, Academic Press, Inc, San Diego, CA, 1994.
[41] A.C. Wright, G. Dalba, F. Rocca, N.M. Vedishcheva, Borate versus silicate glasses: why are they so different? Phys. Chem. Glasses 51 (2010) 233.
[42] J.F. Stebbins, J. Wu, L.M. Thompson, Interactions between network cation coordination and non-bridging oxygen abundance in oxide melts and glasses: insights from NMR spectroscopy, Chem. Geol. 346 (2013) 34.
[43] J.F. Stebbins, W.R. Panero, J.R. Smyth, D.J. Frost, Forsterite, wadsleyite, and ringwoodite (Mg_2SiO_4): ^{29}Si NMR constraints on structural disorder and effects of paramagnetic impurity ions, Am. Mineral. 94 (2009) 626.
[44] S. Sen, J.F. Stebbins, Phase separation, clustering and intermediate range order in $Li_2Si_4O_9$ glass: a ^{29}Si MAS NMR spin-lattice relaxation study, Phys. Rev. 50 (1994) 822.
[45] J.B. Murdoch, J.F. Stebbins, I.S.E. Carmichael, High-resolution ^{29}Si NMR study of silicate and aluminosilicate glasses: the effect of network-modifying cations, Am. Mineral. 70 (1985) 332.
[46] H. Maekawa, T. Maekawa, K. Kawamura, T. Yokokawa, The structural groups of alkali silicate glasses determined from ^{29}Si MAS-NMR, J. Non-Cryst. Solids 127 (1991) 53.
[47] S. Sen, R.E. Youngman, NMR study of Q-speciation and connectivity in K_2O-SiO_2 glasses with high silica content, J. Non-Cryst. Solids 331 (2003) 100.
[48] W.J. Malfait, W.E. Halter, Y. Morizet, B.H. Meier, R. Verel, Structural control on bulk melt properties: single and double quantum ^{29}Si NMR spectroscopy on alkali-silicate glasses, Geochim. Cosmochim. Acta 71 (2007) 6002.
[49] J.F. Stebbins, N. Kim, M.J. Andrejcak, P.M. Boymel, B.K. Zoitos, Characterization of phase separation and thermal history effects in magnesium silicate glass fibers by NMR spectroscopy, J. Am. Ceram. Soc. 92 (2009) 68.
[50] Y. Kawamoto, M. Tomozawa, Prediction of immiscibility boundaries of the systems K_2O-SiO_2, K_2O-Na_2O-SiO_2, and K_2O-BaO-SiO_2, J. Am. Ceram. Soc. 64 (1981) 289.
[51] S.S. Kim, T.H. Sanders Jr., Thermodynamic modeling of phase diagrams in binary alkali silicate systems, J. Am. Ceram. Soc. 74 (1991) 1833.
[52] M.E. Brandriss, J.F. Stebbins, Effects of temperature on the structures of silicate liquids: ^{29}Si NMR results, Geochim. Cosmochim. Acta 52 (1988) 2659.
[53] B.O. Mysen, J.D. Frantz, Raman spectroscopy of silicate melts at magmatic temperatures: Na_2O-SiO_2, K_2O-SiO_2 and Li_2O-SiO_2 binary compositions in the temperature range 25-1475°C, Chem. Geol. 96 (1992) 321.
[54] Y. Xiao, R.J. Kirkpatrick, Y.J. Kim, Investigations of MX-1 tridymite by ^{29}Si MAS NMR; modulated structures and structural phase transitions, Phys. Chem. Mineral. 22 (1995) 30.
[55] H. Graetsch, I. Topalovic-Dierdorf, ^{29}Si MAS NMR spectrum and superstructure of modulated tridymite L3-T0(MX-1), Eur. J. Mineral. 8 (1996) 103.
[56] K. Geisinger, N.L. Ross, P. McMillan, A. Navrotsky, $K_2Si_4O_9$: energetics and vibrational spectra of glass, sheet silicate, and wadeite-type phases, Am. Mineral. 72 (1987) 984.
[57] E.I. Morin, J.F. Stebbins, Separating the effects of composition and fictive temperature on Al and B coordination in Ca, La, Y aluminosilicate, aluminoborosilicate, and aluminoborate glasses, J. Non-Cryst. Solids 432 (2016) 384.
[58] J. Wu, J.F. Stebbins, Cation field strength effects on boron coordination in binary borate glasses, J. Am. Ceram. Soc. 97 (2014) 2794.
[59] J.E. Shelby, Thermal expansion of mixed-alkali silicate glasses, J. Appl. Phys. 47 (1976) 4489.
[60] N.V. Borisova, V.M. Ushakov, M.M. Shultz, Heat capacity, fictive temperature, and degrees of structural and energy ordering in vitreous potassium silicates in relation with their structure, Glas. Phys. Chem. 25 (1999) 408.
[61] M. Ueno, M. Misawa, K. Suzuki, On the change in coordination of Ge atoms in Na_2O-GeO_2 glasses, Physica 120B (1983) 347.
[62] G. Wolf, D.J. Durben, P. McMillan, High-pressure Raman spectroscopic study of sodium tetrasilicate ($Na_2Si_4O_9$) glass, J. Chem. Phys. 93 (1990) 2280.
[63] G.H. Wolf, P.F. McMillan, J.F. Stebbins, P.F. McMillan, D.B. Dingwell (Eds.), Structure, Dynamics, and Properties of Silicate Melts, Mineralogical Society of America, Washington, D.C., 1995, p. 505.
[64] J.L. Yarger, K.H. Smith, R.A. Nieman, J. Diefenbacher, G.H. Wolf, B.T. Poe, P.F. McMillan, Al coordination changes in high-pressure aluminosilicate liquids, Science 270 (1995) 1964.
[65] S.K. Lee, G.D. Cody, Y. Fei, B.O. Mysen, The effect of Na/Si ratio on the structure of sodium silicate and aluminosilicate glasses quenched from melts at high pressure: a multi-nuclear (Al-27, Na-23, O-17) 1D and 2D solid-state NMR study, Chem. Geol. 229 (2006) 162.
[66] S.K. Lee, Y. Fei, G.D. Cody, B.O. Mysen, Order and disorder in sodium silicate glasses and melts at 10 GPa, Geophys. Res. Lett. 30 (2003) 1845.
[67] J.R. Allwardt, J.F. Stebbins, B.C. Schmidt, D.J. Frost, J. Chen, Y. Wang, T.S. Duffy, G. Shen, L.F. Dobrzhinetskaya (Eds.), Frontiers of High Pressure Research, Elsevier, Amsterdam, 2005, p. 211.
[68] L.-S. Du, J.R. Allwardt, B.C. Schmidt, J.F. Stebbins, Pressure-induced structural changes in a borosilicate glass-forming liquid: boron coordination, non-bridging oxygens, and network ordering, J. Non-Cryst. Solids 337 (2004) 196.
[69] E.M. Stolper, T.J. Ahrens, On the nature of pressure-induced coordination changes in silicate melts and glasses, Geophys. Res. Lett. 14 (1987) 1231.
[70] J.F. Stebbins, S.E. Ellsworth, Temperature effects on structure and dynamics in borate and borosilicate liquids: high-resolution and high-temperature NMR results, J. Am. Ceram. Soc. 79 (1996) 2247.
[71] T.J. Kiczenski, L.-S. Du, J.F. Stebbins, The effect of fictive temperature on the structure of E-glass: a multinuclear NMR study, J. Non-Cryst. Solids 351 (2005) 3571.
[72] J. Wu, J.F. Stebbins, Quench rate and temperature effects on boron coordination in aluminoborosilicate melts, J. Non-Cryst. Solids 356 (2010) 2097.
[73] J. Wu, J.F. Stebbins, Temperature and modifier cation field strength effects on aluminoborosilicate glass network structure, J. Non-Cryst. Solids 362 (2013) 73.
[74] E.I. Morin, J.F. Stebbins, Multinuclear NMR investigations of temperature effects on structural reactions involving non-bridging oxygens in multicomponent oxide glasses, J. Non-Cryst. Solids 471 (2017) 179.
[75] J.F. Stebbins, Temperature effects on the network structure of oxide melts and their consequences for configurational heat capacity, Chem. Geol. 256 (2008) 80.
[76] C.T. Moynihan, A.J. Easteal, M.A. DeBolt, J. Tucker, Dependence of the fictive temperature of glass on cooling rate, J. Am. Ceram. Soc. 59 (1976) 12.
[77] I. Farnan, J.F. Stebbins, The nature of the glass transition in a silica-rich oxide melt, Science 265 (1994) 1206.
[78] K.S. Pitzer, L. Brewer, Thermodynamics, McGraw-Hill, New York, 1961.
[79] G.N. Greaves, S. Sen, Inorganic glasses, glass-forming liquids and amorphizing solids, Adv. Phys. 56 (2007) 1.
[80] H. Schweinsberg, F. Liebau, The crystal structure of $K_4[Si_8O_{18}]$: a new type of layer silicate, Acta Cryst. B B30 (1974) 2206.
[81] L.V. Woodcock, C.A. Angell, P. Cheeseman, Molecular dynamics studies of the vitreous state: simple ionic systems and silica, J. Chem. Phys. 65 (1976) 1565.
[82] J. Dickinson Jr., C.M. Scarfe, P. McMillan, Physical properties and structure of $K_2Si_4O_9$ melt quenched from pressures up to 2.4 GPa, J. Geophys. Res. 95 (1990) 15675.
[83] R.A. Lange, I.S.E. Carmichael, J. Nicholls, K. Russell (Eds.), Quantitative Methods in Igneous Petrology, Min. Soc. Amer., Washington, 1990, p. 25.
[84] M.S. Ghiorso, An EOS for silicate melts. III. Analysis of stoichiometric liquids at elevated pressure: shock compression data, molecular dynamics simulations and mineral fusion curves, Am. J. Sci. 304 (2004) 752.
[85] G.B. Martin, F.J. Spera, M.S. Ghiorso, D. Nevins, Structure, thermodynamic, and transport properties of molten Mg_2SiO_4: dynamics simulations and model EOS, Am. Mineral. 94 (2009) 693.
[86] A.C. Hannon, D. DiMartino, L.F. Santos, R.M. Almeida, Ge-O coordination in cesium germanate glasses, J. Phys. Chem. B 111 (2007) 3342.
[87] U. Hoppe, R. Kranold, H.-J. Weber, J. Neuefeind, A.C. Hannon, The structure of potassium germanate glasses-a combined x-ray and neutron scattering study, J. Non-Cryst. Solids 278 (2000) 99.
[88] H. Verweij, J.H.J.M. Buster, The structure of lithium, sodium and potassium germanate glasses, studied by Raman scattering, J. Non-Cryst. Solids 34 (1979) 81.
[89] T. Furukawa, W.W. B., Raman spectroscopic investigation of the structure and crystallization of binary alkali germanate glasses, J. Mat. Sci. 15 (1980) 1648.
[90] G.S. Henderson, H.M. Wang, Germanium coordination and the germanium anomaly, Eur. J. Mineral. 14 (2002) 733.
[91] S.K. Lee, B.H. Lee, Atomistic origin of germanate anomaly in GeO_2 and Na-germanate glasses: insights from two-dimensional ^{17}O NMR and quantum chemical calculations, J. Phys. Chem. B 110 (2006) 16408.
[92] L.S. Du, J.F. Stebbins, Oxygen sites and network coordination in sodium germanate glasses and crystals: high-resolution oxygen-17 and sodium-23 NMR, J. Phys. Chem. B 110 (2006) 12427.
[93] L. Peng, J.F. Stebbins, Sodium germanate glasses and crystals: NMR constraints on variation in structure with composition, J. Non-Cryst. Solids 353 (2007) 4732.
[94] L.-S. Du, L. Peng, J.F. Stebbins, Germanosilicate and alkali germanosilicate glass structure: new insights from high-resolution oxygen-17 NMR, J. Non-Cryst. Solids 353 (2007) 2910.
[95] P.K. Gupta, M.L. Lui, P.J. Bray, Boron coordination in rapidly cooled and in annealed aluminum borosilicate glass fibers, J. Am. Ceram. Soc. 68 (1985) C82.
[96] R.J. Araujo, Statistical mechanics of chemical disorder: application to alkali borate glasses, J. Non-Cryst. Solids 58 (1983) 201.
[97] T. Yano, N. Kunimine, S. Shibata, M. Yamane, Structural investigation of sodium borate glasses and melts by Raman spectroscopy. II. Conversion between BO_4 and BO_2O^- units at high temperature, J. Non-Cryst. Solids 321 (2003) 147.
[98] P.J. Bray, Structural models for borate glasses, J. Non-Cryst. Solids 75 (1985) 29.
[99] A.H. Silver, P.J. Bray, Nuclear magnetic resonance absorption in glass .1. Nuclear quadrupolar effects in boron oxide, soda-boric oxide, and borosilicate glass, J. Chem. Phys. 29 (1958) 984.
[100] P.J. Bray, J.G. O'Keefe, Nuclear magnetic resonance investigations of the structure of alkali borate glasses, Phys. Chem. Glasses 4 (1963) 37.
[101] V.K. Michaelis, P.M. Aguiar, S. Kroeker, Probing alkali coordination environments in alkali borate glasses by multinuclear magnetic resonance, J. Non-Cryst. Solids 353 (2007) 2582.
[102] J.F. Stebbins, P. Zhao, S. Kroeker, Non-bridging oxygens in borate glasses: characterization by ^{11}B and ^{17}O MAS and 3QMAS, Sol. St. NMR 16 (2000) 9.
[103] W.J. Dell, P.J. Bray, S.Z. Xiao, ^{11}B NMR studies and structural modeling of Na_2O-B_2O_3-SiO_2 glasses of high soda content, J. Non-Cryst. Solids 58 (1983) 1.
[104] A.C. Wright, Borate structures: crystalline and vitreous, Phys. Chem. Glasses 51 (2010) 1.

[105] J.C. Mauro, P.K. Gupta, R.J. Loucks, Composition dependence of glass transition temperature and fragility. II. A topological model of alkali borate liquids, J. Chem. Phys. 130 (2009) 234503.
[106] S. Kroeker, et al., Alkali dependence of tetrahedral boron in alkali borate glasses, Phys. Chem. Glasses 47 (2006) 393.
[107] Y.H. Yun, P.J. Bray, Nuclear magnetic resonance studies of the glasses in the system Na_2O-B_2O_3-SiO_2, J. Non-Cryst. Solids 27 (1978) 363.
[108] G.E. Jellison Jr., S.A. Feller, P.J. Bray, A re-examination of the fraction of 4-co-ordinated boron atoms in the lithium borate glass system, Phys. Chem. Glasses 19 (1978) 52.